

IMECE2006-14626

**STUDY ON HEAT TRANSFER AND FLOW BEHAVIOR OF MINI-TUBE BANK FOR  
MICRO HEAT EXCHANGER****Y. Koizumi****Department of Mechanical Engineering  
Kogakuin University  
2665-1, Nakano-machi, Hachioji, 192-0015  
Tokyo, Japan  
koizumiy@cc.kogakuin.ac.jp****T. Okuyama****Department of Mechanical Engineering  
Kogakuin University  
2665-1, Nakano-machi, Hachioji, 192-0015  
Tokyo, Japan****H. Ohtake****Department of Mechanical  
Engineering  
Kogakuin University  
2665-1, Nakano-machi, Hachioji,  
192-0015 Tokyo, Japan  
at10988@ns.kogakuin.ac.jp****ABSTRACT**

Heat transfer and flow behavior in the mini tube bank were examined. The tube bank was composed of 1 mm diameter nickel wires and a 30 mm wide  $\times$  15 mm high flow channel. Experiments were performed in the range of the rod  $Re = 5 \sim 430$  by using water. Numerical analyses were also conducted with the commercial CFD code STAR-CD. The heat transfer coefficient after the second row was lower than first row's one. The flow visualization results indicated that the wake region was stagnant when the Reynolds number was low. This flow stagnation seemed to cause the heat transfer coefficient deterioration in the tube bank. As the Reynolds number was increased, the flow state in the wake region gradually changed from the stagnant condition to the more disturbed condition. The deeper the row was, the more disturbed the wake was. The heat transfer coefficient began to recover to the first row value at certain Reynolds number. The recovery started from the most downstream row; fifth row in the present experiments and was propagated to the upstream row. The Reynolds number when the recovery was initiated decreased as the spacing between rods was increased. The analytical results of the STAR-CD code supported the experimental results. When the wake was stagnant, the heat transfer coefficient distribution around the rear rod, i.e. the rod in the wake, showed a large dip in the front

region of the rod. It was considered that this dip caused the heat transfer coefficient decrease after the second row observed in the experiments.

**INTRODUCTION**

Heat exchangers are one of the main pieces of equipments for engineering systems such as power plants, chemical plants and so on. They have been investigated by many researchers from many aspects. An effort has been made to improve the efficiency of heat exchangers pursuing more efficient energy use. One of these efforts is to adopt small diameter tubes and small fins.

Kamisaka et al. [1] examined the effect of micro needle fins formed on the tubes of the heat exchanger on the heat transfer and developed the correlation of the heat transfer coefficient.

A heat transfer coefficient across a tube increases as the tube diameter is decreased. It implies that when the tube diameter and the size of the heat exchanger are scaled down, the overall heat transfer coefficient and the efficiency would be enhanced. Kasagi et al. [2, 3] examined micro-bare tube heat exchangers to improve the heat exchanger efficiency. They

provided the design guide line for these micro heat exchangers from numerical analyses.

The flow patterns through a tube bank are so complicated that it is virtually impossible to predict heat transfer and pressure drop by numerical analysis [4]. Therefore, an experimental approach is the only alternative and a lot of experimental data are available in the literature. In the turbulent condition of the tube bank, turbulence created by the preceding row has an effect on the heat transfer of the following row. Heat transfer is usually improved as the tube row proceeds deep [5]. However, that effect depends on the tube spacing. When the tube spacing becomes narrow, heat transfer is deteriorated [6].

When the tube size is scaled down to miniature size to improve the heat transfer coefficient, the flow becomes laminar. The heat transfer coefficient of a tube bank is 50 % lower than that of the first row [4]. Mochizuki et al. [7] and Yagi and Mochizuki [8] examined heat transfer and pressure drop of the miniature size rod bank. They reported that the heat transfer coefficient of the rod bank could be larger than that of the single rod in some case. It was pointed out that the heat transfer coefficient of the rod bundle is highly sensitive to the flow state and it was complicatedly affected by the rod arrangement.

It is considered that flow and heat transfer data on the mini-size tube bank are still required to get better design guideline for micro heat exchangers. It seems important to examine the flow state in the wake region between the front and rear tubes.

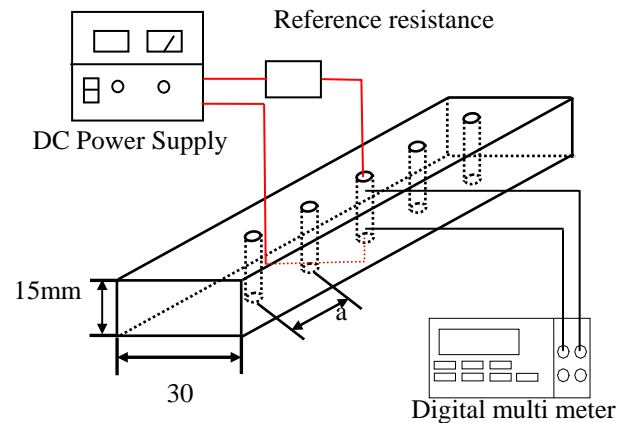


Fig. 2 Details of test section

In the present paper, the flow behavior and the heat transfer of the 1 mm diameter tube bank were experimentally examined. Fluid used was distilled water. The test condition covered the Reynolds number from 5 to 430. Experimental results were also analyzed with a commercial analytical code of STAR-CD.

## EXPERIMENTAL APPARATUS AND TEST PROCEDURES

### Experimental Apparatus

An apparatus used in the present study is schematically shown in Fig. 1. It consists of a water tank, a circulation pump, rotameters, a calming grid at the inlet of the test section, a test section and a low-voltage DC current supply system.

The test section is made of transparent Plexiglas. The length is 480 mm and the cross-section is 30 mm wide and 10 mm high. It has the calming grid at the inlet that is composed of 3 mm cell-size octagonal pipes of 300 mm long. The test tube bank is located 10 mm downstream from the calming grid.

The outline of the test tube bank used in the present experiments is illustrated in Fig. 2. The tube is simulated with a 1 mm diameter nickel wire. Five wires are arranged in a straight line with a specified pitch.

Distilled water in the water tank was cleaned with a strainer prior to each experiment by circulating water by using the bypass line. After water was cleaned, the strainer was isolated. Then, water flow was directed to the test section through the flowmeter and the temperature measuring section with a K-type thermocouple. The water flow went into the test tube bank section through the calming grid section. A differential pressure between the inlet and the outlet of the tube bank was measured by an Hg manometer. Water from the test section returned to the tank.

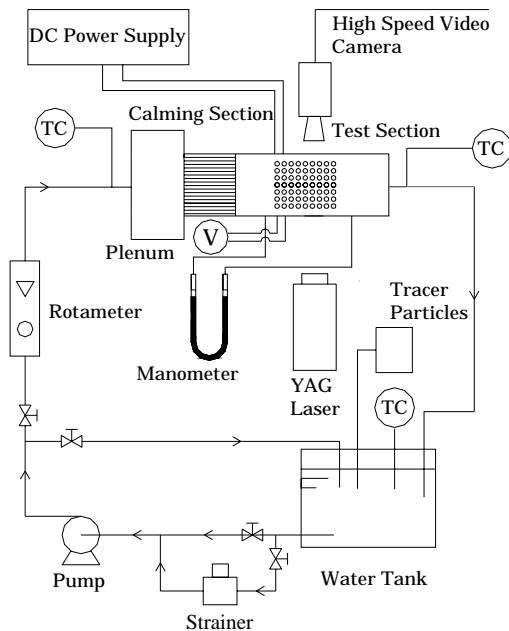


Fig.1 Experimental Apparatus

### Heat Transfer Experiment Procedure

Low voltage DC current was supplied to one nickel wire to heat it. The wire was heated by joule heating. It depended upon a test condition which wire was heated. Two alumel wires of 0.1 mm diameter were spot-welded on the heated nickel wire with an interval of 6 mm. The DC current supplied and the voltage between the spot-welded alumel wires were measured. Electric power supplied to the wire was derived from the current and the voltage, and then changed the heating rate. Electric resistance was also calculated from the current and the voltage. By referring to the relation between the electric resistance and the wire temperature that had been calibrated prior to the experiment, mean wire temperature was obtained.

For the fixed flow rate and the fixed rod spacing, five experiments were iterated; first wire was heated, second wire was heated, and so on.

The pitch between the neighboring wires were varied from  $a/d = 2$  through 9. Here,  $a$  is the distance between centers of neighboring wires and  $d$  is the wire diameter. Water temperature at the inlet of the test section was 20 °C. The water velocity upstream of the wires in the test section was varied in the range of 0.0036 ~ 0.34 m/s and the flow conduit Reynolds number of  $10^4 \sim 10^5$ , which corresponded to the wire Reynolds number =  $u_0 d / \nu$  of 5 ~ 430. Here,  $u_0$  is the water velocity upstream of the wires in the test section and  $d$  is the diameter of the wire.

### Flow Visualization Experiment Procedure

Fluorescent dye of 6 μm diameter particles was dissolved in distilled water as tracer particles. A YAG laser sheet was emitted from the side of the tube bank. The visualized flow image was recorded from the top of the test section by a high speed video camera with a frame rate of 60 ~ 500 f/s. The recorded pictures went through the binary digitizing process, and then the velocity field was determined by the PIV method.

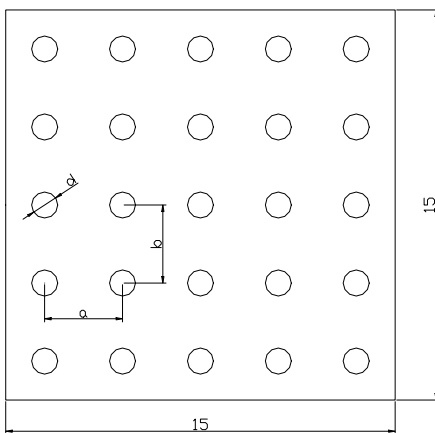


Fig.3 Analysis model

### NUMERICAL ANALYSES WITH STAR-CD

The flow field in the rod bank of a 5×5 array, shown in Fig. 3, was analyzed two-dimensionally with the STAR-CD code. Fluid was water as in the experiments. Water flows from left to right across the rod bank in the figure. The rod diameter  $d$  was 1 mm and the flow direction pitch  $a$  and the vertical direction pitch  $b$  were 3 mm, respectively.

### RESULTS AND DISCUSSIONS

#### Single Rod Results

Heat transfer results of the case that only one wire (one rod) was placed in the test section are presented in Fig. 4. The Nusselt number is defined in the figure as

$$Nu = \frac{hd}{k} \quad (1)$$

where  $d$  is the wire (rod) diameter,  $h$  is the mean heat transfer coefficient of the wire (rod) and  $k$  is the thermal conductivity. The mean heat transfer coefficient was derived in the experiments as follows:

$$h = \frac{q_w}{(T_w - T_0)} \quad (2)$$

where  $q_w$  is the mean nickel wire surface heat flux derived from the wire heating rate,  $T_w$  is the mean nickel wire temperature and  $T_0$  is the water temperature.

In Fig. 4, analytical results by the STAR-CD code and values calculated with the McAdams correlation [5]

$$\frac{hd}{k_f} = C Re_f^n Pr_f^{1/3} \quad (3)$$

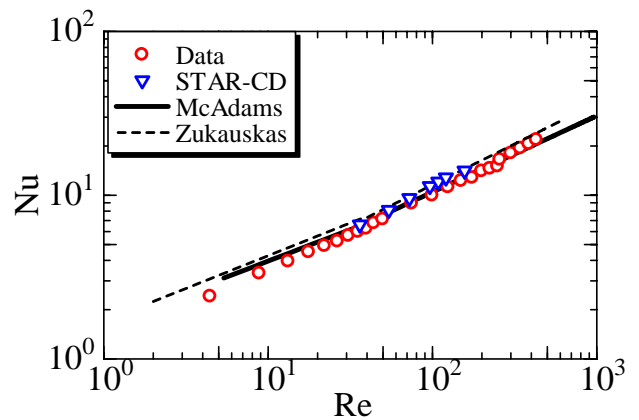


Fig.4 Heat transfer coefficient (Single rod case)

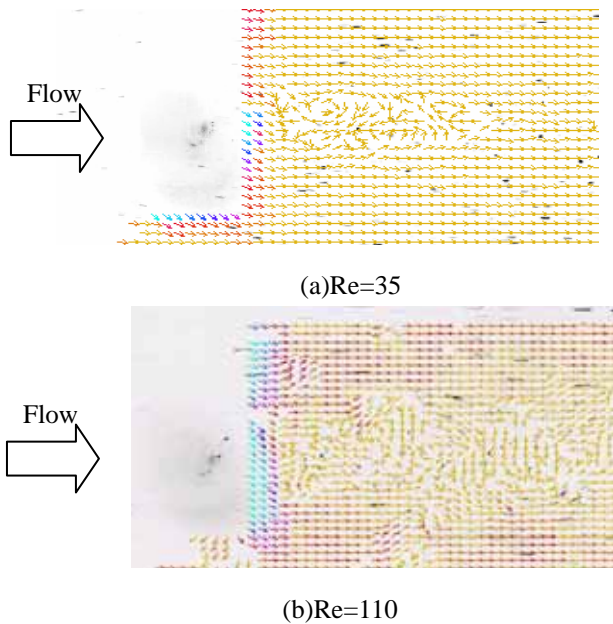


Fig.5 Measured flow field (Single rod case)

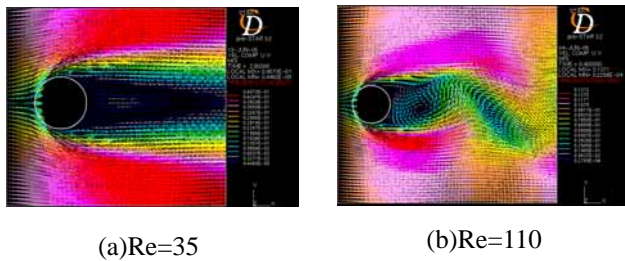


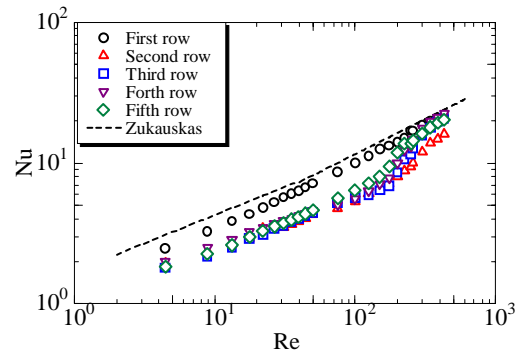
Fig.6 STAR-CD analysis (Single rod case)

and the Zukauskas correlation [9]

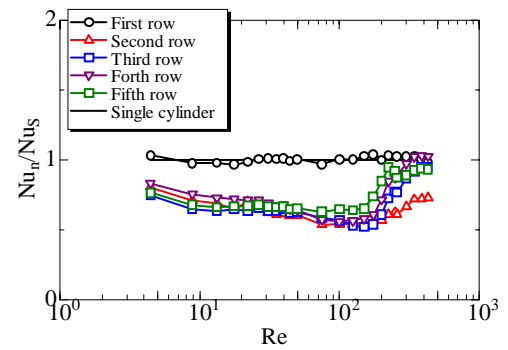
$$Nu_m = C_1 Re^n Pr^{0.37} \left( \frac{Pr}{Pr_w} \right)^{0.25} \quad (4)$$

are also included for comparison. Both correlations predicted well the experimental results. The STAR-CD analytical results also agree well with the measured results.

The velocity fields obtained in the experiments by the PIV method are illustrated in Fig. 5. As expected, two patterns of vortices were observed. In Fig. 5 (a), the wire Reynolds number is  $Re = 35$ . Twin vortices are clearly seen in the wake region. The vortices steadily existed. This situation was observed in the range of  $Re = 10 \sim 50$ .

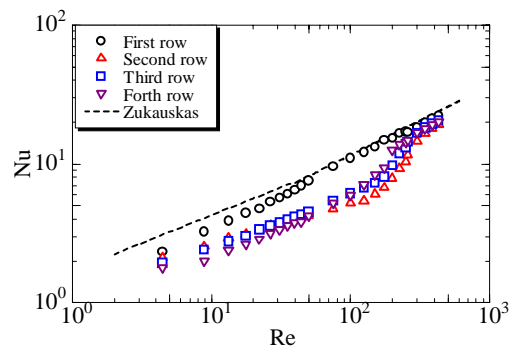


(a) Nusselt number

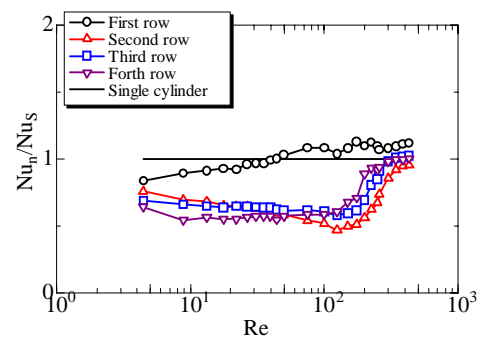


(b) Heat transfer deterioration

Fig.7 Heat transfer coefficient ( $a/d = 3$ )

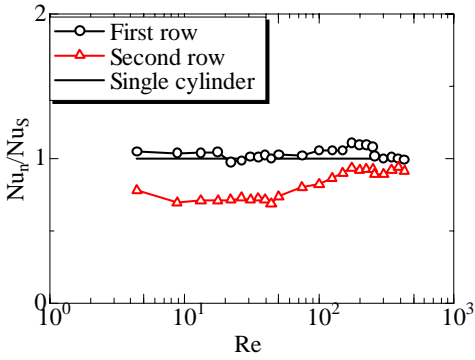


(a) Nusselt number

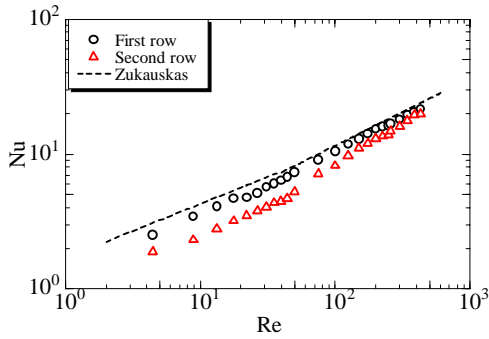


(b) Heat transfer deterioration

Fig.8 Heat transfer coefficient ( $a/d = 4$ )



(a) Nusselt number



(b) Heat transfer deterioration

Fig.9 Heat transfer coefficient ( $a/d = 9$ )

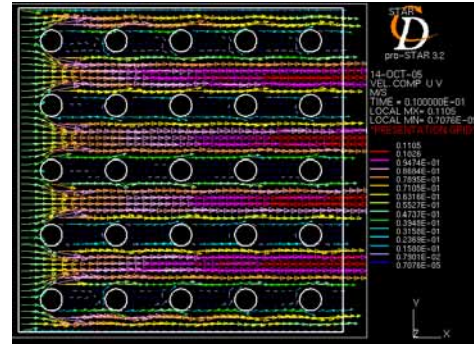


Fig. 11 Velocity distribution (STAR-CD,  $Re = 85$ )

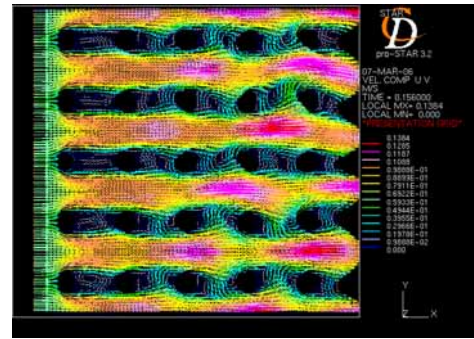


Fig. 12 Velocity distribution (STAR-CD,  $Re = 110$ )

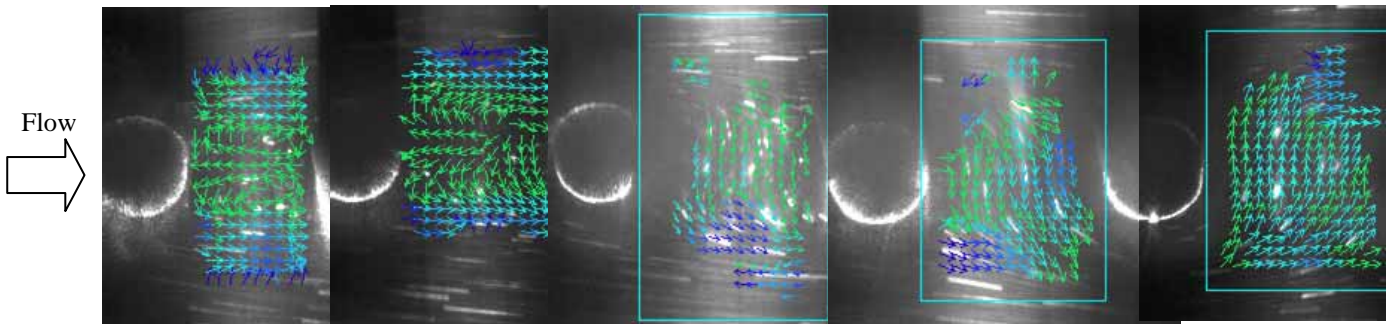


Fig.10 Measured flow field  
( $a/d=3$ )

As the Reynolds number was increased, the twin vortices became gradually unstable and periodical vortex shedding (the Karman vortex) was eventually initiated at  $Re \geq 60$  as shown in Fig. 5 (b).

These trends agree well with the STAR-CD analysis results as shown in Fig. 6.

### Rod Bank Results

Heat transfer experiment results obtained in the in-line five-row arrangement of rods (wires) are presented in Figs. 7, 8

and 9. In these figures, figure (a) expresses heat transfer coefficients in the form of the Nusselt number. In figure (b), these values are normalized by using the Zukauskas correlation values for each condition.

It is clearly observed in Fig. 7 that the heat transfer coefficient decreases as flow goes downstream. This fact contradicts the handbook knowledge of the usual size heat exchanger that the heat transfer coefficient increases as flow goes downstream and the increasing saturates around the 10th row [9]. There, the flow is usually turbulent and the rod Reynolds number is larger than  $10^3$ . Here, however, the

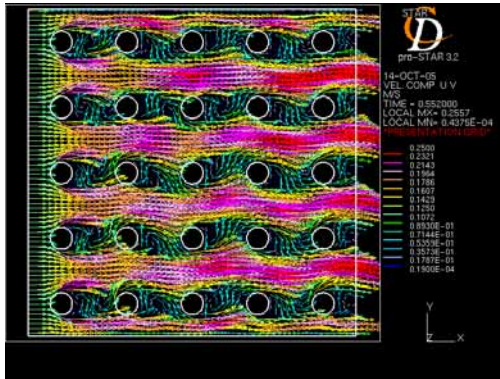
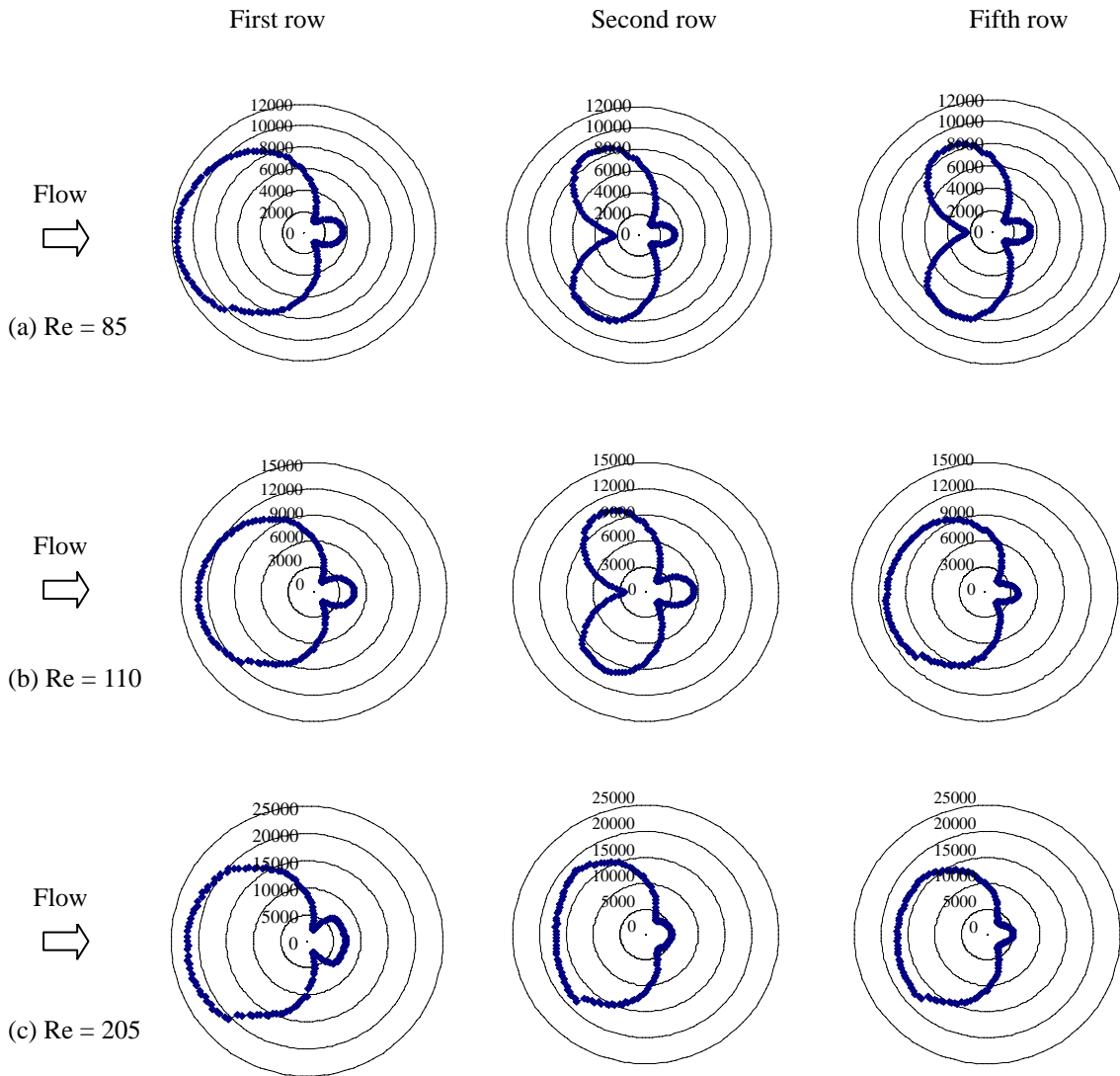


Fig. 13 Velocity distribution (STAR-CD,  $Re = 205$ )

Reynolds number is less than  $10^3$ . It seems that the deeper the row is, the larger the decrease is. As the Reynolds number increases, the heat transfer coefficient begins to recover and it reaches back to the first row value. This recovery occurs from the deepest row and is propagated upstream. The Reynolds number where the heat transfer coefficient turns to recover to the first row value seems to decrease as the distance between rods becomes wider. Even in the case that the distance between the rods is largest in the present experiments;  $a/d = 9$ , the heat transfer coefficient decrease occurred as shown in Fig. 9. It should be noticed that it is usually said that the wake region length is approximately  $5d$  in the turbulent condition. Visualized flow states by the PIV method are presented in Fig. 10. The conditions shown in the figure are  $a/d = 3$  and  $Re = 180$ . The flow direction in the figure is from left to right. In the



Note: Numbers in the figure are heat transfer coefficients  $W/m^2$ .

Fig. 14 Local heat transfer coefficients

wake behind the first row, the stagnant and slow velocity field is observed. In the second row wake, the flow begins to fluctuate. In the third row wake, vortices are periodically shedding. Same flow states are observed in the fourth and fifth row wakes. The Reynolds numbers when the vortex shedding starts are 200, 180, 170 and 100 in the second, the third, the fourth and the fifth row wake. These Reynolds numbers well correspond to the Reynolds number where the heat transfer coefficient begins to recover in Fig. 7 although the vortex shedding is not observed in the first row wake. These facts suggest that the heat transfer coefficient decrease in the rod bank has something to do with the stagnant and slow velocity field of the wake.

Velocity fields in the 5×5 tube bank predicted with the STAR-CD code are presented in Figs. 11 ~ 13. The flow direction in the figure is from left to right. When  $Re = 85$  in Fig. 11, the flow behind a rod seems stagnant and very slow in almost all rows. It should be noticed that when there is only one rod in the flow field, Karman vortices were observed in the wake region. When  $Re = 110$  in Fig. 12, the vortex shedding starts from the third row. When  $Re = 205$  in Fig. 13, the vortex shedding is noticed in all rows. The fluctuating and disturbed state becomes more prominent as the flow goes downstream. These results well correspond to the observed results shown in Fig. 10.

Heat transfer coefficient distributions around a rod are presented in Fig. 14. The distribution profiles of the first row are approximately similar in all cases irrespective of the Reynolds number. However, when  $Re = 85$ , there is a large dip at the stagnation point of and after the second row rod. This dip is only observed on the second row rod when  $Re = 110$ . When  $Re = 205$ , there is no dip on the rear rod and the heat transfer coefficient distribution profiles are almost same on the all row rod. It could be concluded that the flow stagnation and slow velocity field behind the rod cause the low heat transfer coefficient on the rear rod.

## CONCLUSIONS

Heat transfer and flow behavior in the mini rod bank were examined. The tube bank was composed of 1 mm diameter wires and a 30 mm wide × 15 mm high flow channel. Experiments were performed in the range of the rod  $Re = 5 \sim 430$ . Numerical analyses were also conducted with the commercial CFD code STAR-CD. Conclusions obtained are as follows.

(1) In usual size tube banks ( $Re > 10^3$ ), a heat transfer coefficient increases as the tube row goes downstream. However, the measured heat transfer coefficient after the second row was lower than the first row. The flow visualization results indicated that the wake region was stagnant. This flow stagnation seemed to cause the heat transfer coefficient deterioration.

(2) As the Reynolds number was increased, the flow state in the wake region gradually changed from the stagnant condition to the more disturbed condition. The deeper the row

was, the more disturbed the wake flow state was. The heat transfer coefficient began to recover to the first row value at certain Reynolds number. The recovery started from the most downstream row; fifth row in the present experiments and was propagated to the upstream row. The Reynolds number when the recovery was initiated decreased as the spacing between rods was increased.

(3) The analytical results of the STAR-CD code supported the experimental results. When the Reynolds number was low, the flow state in the wake region was stagnant. As the Reynolds number was increased, the wake condition gradually changed from the stagnant condition to the more disturbed condition and it started from the most downstream row. When the wake was stagnant, the heat transfer coefficient distribution around the rear rod showed a large dip in the front region of the rod. It was considered that this dip caused the heat transfer coefficient decrease after the second row as observed in the experiments.

## REFERENCES

- [1] Kamisaka, M., Aoki, Y. and Ueda, S., 1988. "Heat Transfer Characteristics of Pin-Finned Heat Exchangers", Proc. 25th National Heat Transfer Symp. of Japan, Vol. 1, 181-183.
- [2] Kasagi, N., Shikazono, N., Suzuki, Y. and Oku, T., 2003. "Assessment of High-Performance Micro Bare-Tube Heat Exchangers for Electronic Equipment Cooling", Proc. 1st Int. Symp. on Process Intensification and Miniaturization, Univ. of Newcastle upon Tyne, UK, CD-ROM.
- [3] Kasagi, N., Shikazono, N., Suzuki, Y. and Oku, T., 2003. "Optimal Design and Assessment of High-Performance Micro Bare-Tube Heat Exchangers", Proc. 4th Conf. on Compact Heat Exchangers and Enhancement Technology for the Process Industries, Crete Island, Greece, 241 - 246.
- [4] Özisik, M. N., 1987. "Basic Heat Transfer", Robert E. Krieger Publishing Co., 278 - 282.
- [5] Katto, Y., 1964. "Heat Transfer Introduction", Yokendo Co., 155 - 156, 158 - 160.
- [6] Rohsenow, W. M., Hartnett, J. P. and Ganic, E. N., 1973. "Handbook of Heat Transfer Fundamentals", McGraw-Hill Book Co., 7-110 - 7-116.
- [7] Mochizuki, S., Yagi, Y. and Hara, T., 1992. "Heat Transfer and Pressure Drop Performance of Wire-Fin Surfaces", Trans. JSME, Vol. 58, No. 566, 3729 -3734.
- [8] Yagi, Y. and Mochizuki, S., 1994. "Empirical Correlation for Heat Transfer and Pressure Drop Characteristics of Thin Wire Fin Surfaces", Trans. JSME, Vol. 60, No. 575, 2518 - 2523.
- [9] JSME, 1986. "Heat Transfer Materials", JSME, 64 - 65.